Polymer Chemistry

Cite this: *Polym. Chem.*, 2012, **3**, 640

www.rsc.org/polymers

PAPER

Bioinspired dual self-folding of single polymer chains *via* reversible hydrogen bonding†

Ozcan Altintas,[a] Elise Lejeune,[ab] Peter Gerstel[a] and Christopher Barner-Kowollik*[ab]

Received 2nd September 2011, Accepted 9th October 2011
DOI: 10.1039/c1py00392e

With the long term aim of preparing synthetic macromolecules that mimic the folding actions of natural biomacromolecules, a single synthetic polymer chain containing two distinct and orthogonal hydrogen bonding recognition motifs has been synthesized using an atom transfer radical polymerization (ATRP) and orthogonal ligation strategy. The hydrogen bonding recognition units, based on both three-point thymine (Thy)–diaminopyridine (DAP) and six-point cyanuric acid (CA)–Hamilton wedge (HW) interactions, induced—at low concentrations—a single chain self-folding process. The self-assembly process was monitored—initially between small molecule models—by proton nuclear magnetic resonance (^{1}H NMR) spectroscopy, revealing full orthogonality of the two recognition pairs, HW–CA and Thy–DAP. Dynamic as well as static light scattering (DLS and SLS) analyses of the macromolecular self-assembly systems provide unambiguous evidence for the hydrogen-bonding interactions between both the Thy–DAP and CA–HW units leading to well-defined dual point single chain self-folding, indicating that more complex single chain self-assemblies based on synthetic polymers should be able to mimic—on a simplified level—the folding actions of natural biomacromolecules. The reversibility of the self-folding action depends on temperature as confirmed *via* ^{1}H-NMR spectroscopy in [D_2]tetrachloroethane.

Introduction

The emulation of natural processes and the design of chemical reaction sequences inspired by nature is—or at least should be—one of the most important driving forces for synthetic macromolecular design. Reversible self-folding processes are nature's way to control the conformation of biological polymers. Many proteins undergo folding in solution to yield delicate molecular assemblies stabilized by non-covalent or—in some case—covalent interactions.[1–4] Recently, a wide array of synthetic approaches has been designed to conjugate synthetic macromolecules with biological entities, *e.g.* peptides and proteins,[5–7] with a view to employing them as drug or gene delivery vectors.[8,9] Many of these approaches make use of radical polymerization processes that feature living characteristics[10–12] combined with modular conjugation protocols,[13] some of which fulfil the criteria of a *click* reaction.[14,15] While such approaches are highly notable, they do not emulate naturally occurring molecules in the strict sense yet rather aim at imparting additional specific characteristics to biomolecules that aid in fulfilling their function within a defined biological context. Only very recently have attempts been made to emulate the folding behavior of natural biomacromolecules—such as proteins—on a simple level, yet based entirely on synthetic polymeric systems.[16–19] The key binding principle in nature revolves around the formation of reversible hydrogen bonds between suitable hydrogen donor and acceptor systems. Thus, it seems appropriate to transfer this concept when attempting to fold synthetic macromolecules to mimic naturally occurring systems. In addition, hydrogen bond-mediated self-assembly is a powerful strategy within supramolecular polymer chemistry.[20,21] Hydrogen donor/acceptor systems have featured strongly in polymer chemistry—especially over the last decade—and have been employed to construct reversibly forming block copolymers,[22–28] star polymers,[29–33] cyclic polymers[34] and nanoparticles.[35–40] Biomolecules typically entail several hydrogen donor/acceptor systems, which lead to the formation of specific tertiary structures that enable the biomolecules to fulfil a certain function. Importantly, biomolecules undergo single chain folding without the participation of other (identical) biomolecule entities. In the present contribution, we generate for the first time—based on our earlier results of a single chain entropy driven circular α,ω-self-folding—a well-defined synthetic

[a]*Preparative Macromolecular Chemistry, Institut für Technische Chemie und Polymerchemie, Karlsruhe Institute of Technology (KIT), Engesserstr. 18, 76128 Karlsruhe, Germany. E-mail: christopher.barner-kowollik@kit.edu; Web: www.macroarc.de*
[b]*Soft Matter Synthesis Laboratory, Institut für Biologische Grenzflächen I, Karlsruhe Institute of Technology (KIT), Herrmann-von-Helmholtz-Platz 1, 76344, Eggenstein-Leopoldshafen, Germany*

† Electronic supplementary information (ESI) available: Materials, instrumentation, and mathematical model for determination of K_{ass}, ^{1}H NMR spectra of compounds **2**, **4**, **5**, **8**, **9**, **10**, **11**, and **14**, as well as a Zimm-Plot (SLS) and DLS data of **14**. See DOI: 10.1039/c1py00392e

macromolecule which features two pairs of mutually orthogonal hydrogen bonding motifs (cyanuric acid–Hamilton wedge and thymine–diaminopyridine) at well-defined points within the polymer chains. To achieve the above synthetic aim, we employ atom transfer radical polymerization protocols alongside copper catalyzed [2 + 3] dipolar cycloaddition chemistry. We demonstrate the orthogonal nature of the employed hydrogen binding motifs and evidence—*via* dynamic and static light scattering and ^{1}H-NMR experiments—that the system undergoes strong, entropy-driven single chain self-folding with a high equilibrium constant. The present system thus represents the to-date closest fully synthetic analogue to a biological self-folding macromolecule forming a tertiary structure. Scheme 1 represents the generic nature of the target molecule as well as its entropy driven self-folding action.

Experimental section

The materials section and a detailed description of the analytical instrumentation as well as ^{1}H NMR and of all basis macromolecular compounds can be found in the ESI†.

Synthesis

4-(11-Oxo-11-(6-pivalamidopyridin-2-ylamino)undecyloxy)benzoic acid (**1**),[17] propargyl 2-hydroxymethyl-2-(α-bromoisobutyl oxy methyl)-propionate (**2**),[41] methyl 11-(5-methyl-2,4-dioxo-3,4-dihydropyrimidin-1(2*H*)-yl)undecanoate (**4**),[42] 6-(2,4,6-trioxo-1,3,5-triazinan-1-yl)hexyl 2-bromo-2-methylpropanoate (**7**)[16] and N^1,N^3-bis(6-(3,3-dimethylbutanamido)pyridin-2-yl)-5-(prop-2-ynyloxy)isophthalamide (**13**)[16] were synthesized according to literature procedures.

2-((2-Bromo-2-methylpropanoyloxy)methyl)-2-methyl-3-oxo-3-(prop-2-ynyloxy) propyl 4-(11-oxo-11-(6-pivalamidopyridin-2-ylamino)undecyloxy)benzoate (3). Precursor **1** (1 g, 2.01 mmol) was dissolved in 5 mL dry DMF. Compound **2** (0.516 g, 1.6 mmol) and 4-dimethylaminopyridine (DMAP) (0.025 g, 0.2 mmol) were dissolved in 10 mL of dry DCM and subsequently added to the solution. DCC (0.622 g, 3.01 mmol) was dissolved in 5 mL dry DCM and subsequently added to the mixture. The reaction was carried out at ambient temperature overnight. Solids were filtered off, the filtrate was concentrated and the crude product was purified by column chromatography on silica gel, eluting with *n*-hexane/ethylacetate (2/1) to give the diaminopyridine bearing linker **3** as a viscous liquid (0.874 g, 68%). ^{1}H NMR (400 MHz, DMSO-d_6) δ (ppm) 10.17 (s, 1H), 9.16 (s, 1H), 7.89–7.87 (d, 2H), 7.79–7.71 (m, 2H), 7.61–7.59 (d, 1H), 7.05–7.02 (d, 2H), 4.79 (s, 2H), 4.40 (m, 4H), 4.04 (t, 2H), 3.58 (s, 1H), 2.35 (t, 2H), 1.88 (s, 6H), 1.72 (m, 2H), 1.55 (m, 2H), 1.39–118 (bm, 26H). ^{13}C NMR (100 MHz, DMSO-d_6) δ (ppm) 176.63, 172.16, 171.53, 170.25, 164.80, 162.82, 150.42, 150.13, 139.79, 131.34, 121.07, 114.46, 109.93, 109.10, 77.96, 77.92, 67.84, 66.46, 65.28, 59.71, 56.80, 52.60, 46.42, 40.13, 35.96, 30.07, 28.91, 28.79, 28.70, 28.53, 28.46, 26.88, 25.40, 24.95, 20.72, 17.16, 14.05. ESI-MS (M + Na)$^+$ $C_{40}H_{54}BrN_3O_9$ theoretical: 822.29, experimental: 822.30.

11-(5-Methyl-2,4-dioxo-3,4-dihydropyrimidin-1(2*H*)-yl)undecanoic acid (5). A solution of NaOH (1 N, 10 mL) was added to a solution of compound **4** (2 g, 6.17 mmol) in THF/MeOH (2 : 1, 30 mL). The solution was stirred at ambient temperature for 5 h and subsequently concentrated to a volume of 15 mL. The reaction mixture was poured into 150 mL of water and concentrated HCl was added in a dropwise fashion to generate a white precipitate, which was filtered, washed with water, and dried under vacuum to give compound **5** as a white solid (1.85 g, 97%). ^{1}H NMR (400 MHz, DMSO-d_6) δ (ppm) 11.97 (s, 1H), 11.19 (s, 1H), 7.54 (s, 1H), 3.62 (t, 2H), 2.21 (t, 2H), 1.75 (s, 3H), 1.57–1.48 (bm, 4H), 1.25 (s, 14H). ^{13}C NMR (100 MHz, DMSO-d_6) δ (ppm) 174.45, 164.17, 150.67, 141.49, 108.08, 46.95, 33.47, 28.79, 28.77, 28.66, 28.55, 28.50, 28.38, 28.27, 25.75, 24.45, 11.78. ESI-MS (M + Na)$^+$ $C_{17}H_{28}N_2O_4$ theoretical: 333.2, experimental: 333.3.

2-((2-Bromo-2-methylpropanoyloxy)methyl)-2-methyl-3-oxo-3-(prop-2-ynyloxy) propyl 11-(5-methyl-2,4-dioxo-3,4-dihydropyrimidin-1(2*H*)-yl)undecanoate (6). Precursor **5** (0.5 g, 1.61 mmol) was dissolved in 5 mL dry DMF. Compound **2** (0.414 g, 1.29 mmol) and 4-dimethylaminopyridine (DMAP) (0.02 g, 0.16 mmol) were dissolved in 10 mL dry DCM and subsequently added to the solution. DCC (0.498 g, 2.41 mmol) was dissolved in 5 mL dry DCM and subsequently added to the mixture. The reaction was carried out at ambient temperature overnight. Solids were filtered off, the filtrate was concentrated and the crude product was purified by column chromatography on silica gel, eluting with *n*-hexane/ethylacetate (1/1) to give the thymine bearing linker **6** as a viscous liquid (0.656 g, 83%). ^{1}H NMR (400 MHz, DMSO-d_6) δ 11.19 (s, 1H), 7.53 (s, 1H), 4.75 (s, 2H), 4.26–4.19 (d, 4H), 3.58 (t, 3H), 2.28 (t, 2H), 1.88 (s, 6H), 1.75 (s, 3H), 1.55–1.52 (bm, 4H), 1.49–1.24 (bs, 17H). ^{13}C NMR (100 MHz,

Scheme 1 Mimicking natural protein structures based on two pairs of mutually orthogonal recognition motifs (thymine–diaminopyridine and cyanuric acid–Hamilton wedge) alongside its reversible self-folding process.

DMSO-*d*6) δ (ppm) 172.37, 171.43, 170.19, 164.24, 150.82, 141.39, 108.31, 77.91, 77.87, 66.35, 64.69, 59.57, 56.78, 52.55, 47.08, 46.14, 40.13, 39.92, 39.71, 39.50, 39.29, 39.08, 38.87, 33.46, 33.28, 30.08, 28.79, 28.74, 28.58, 28.39, 28.33, 25.76, 24.41, 24.32, 17.08, 14.05, 11.87. ESI-MS $(M + Na)^+$ $C_{28}H_{41}BrN_2O_8$ theoretical: 635.2, experimental: 635.3.

Synthesis of α-CA-ω-Br functional polystyrene (8). To a 50 mL Schlenk tube, styrene (8.0 mL, 6.98 mmol), PMDETA (73 μL, 0.35 mmol) and **7** (132 mg, 0.35 mmol) in 2 mL of anisole were added and the reaction mixture was degassed by three freeze–pump–thaw cycles and left under argon. CuBr (50 mg, 0.35 mmol) was added to the solution under argon flow. The tube was subsequently placed in a thermostatted oil bath at 110 °C for 30 min. The polymerization mixture was cooled in an ice bath, diluted *via* the addition of THF and the copper catalyst was removed by passing through a short column of neutral alumina. The solvent was removed under reduced pressure, subsequently diluted with the addition of DCM and extracted with EDTA solution to remove Cu (a catalyst also complexed by the recognition unit).[30] The organic phase was dried over Na_2SO_4, concentrated and subsequently precipitated two times into 80 mL methanol. The polymer was dried for 24 h under high vacuum and afforded a white solid (0.87 g). $M_{n,NMR}$ = 3100 Da, $M_{n,SEC}$ = 3000 Da, PDI = 1.06 (end group fidelity close to 100%). The bromide of polymer **8** was subsequently converted to an azide functionality following a literature procedure.[43] ATR-IR (cm^{-1}): 2095 (N_3 stretching). $M_{n,NMR}$ = 3100 Da, $M_{n,SEC}$ = 3000 Da, PDI = 1.06 (end group fidelity 100%).

Synthesis of α-CA-ω-Thy functional polystyrene (9). α-CA-ω-azide polystyrene (820 mg, 0.26 mmol), compound **6** (244 mg, 0.39 mmol), copper(II) sulfate pentahydrate (132 mg, 0.52 mmol) and sodium ascorbate (105 mg, 0.52 mmol) were dissolved in DMF (10 mL). The resulting mixture was stirred at ambient temperature for 24 h. 40 mL of DCM was added to the solution and extracted two times with 10 mL of EDTA solution to remove Cu (a catalyst also complexed by the recognition unit). The organic phase was dried over Na_2SO_4, concentrated and subsequently precipitated twice in 80 mL methanol. The polymer was dried for 24 h in a high vacuum to give a yellowish solid (0.92 g). $M_{n,NMR}$ = 3700 Da, $M_{n,SEC}$ = 3900 Da, and PDI = 1.04 (end group fidelity 98%).

Synthesis of CA-PS-Thy-PS-Br (10). Into a 50 mL Schlenk tube, styrene (6.9 mL, 0.06 mol), PMDETA (12.6 μL, 0.06 mmol) and **9** (223 mg, 0.06 mmol) in 3.45 mL of anisole were added and the reaction mixture was degassed by three freeze–pump–thaw cycles and left under argon. CuBr (8.6 mg, 0.06 mmol) was added to the solution under argon flow. The tube was subsequently placed in a thermostatted oil bath at 110 °C for 60 min. The crude polymer was purified and dried as described above for **8** to give **10** as white solid (473 mg). $M_{n,NMR}$ = 7500 Da, $M_{n,SEC}$ = 7100 Da, and PDI = 1.11 (end group fidelity 90%). Subsequently, the terminal bromide of polymer **10** was converted to the azide functionality as described above for **8**. ATR-IR (cm^{-1}): 2095 (N_3 stretching). $M_{n,NMR}$ = 7900 Da, $M_{n,SEC}$ = 7700 Da, and PDI = 1.11 (end group fidelity 100%).

Synthesis of CA-PS-Thy-PS-DAP (11). CA-PS-Thy-PS-azide (430 mg, 0.054 mmol), compound **3** (65 mg, 0.081 mmol), copper (II) sulfate pentahydrate (27 mg, 0.108 mmol) and sodium ascorbate (21 mg, 0.108 mmol) were dissolved in DMF (10 mL). The resulting mixture was stirred at ambient temperature for 24 h. The crude polymer was purified and dried as described above for **9** to give **11** as white solid (454 mg). $M_{n,NMR}$ = 8700 Da, $M_{n,SEC}$ = 8800 Da, and PDI = 1.11 (end group fidelity 91%).

Synthesis of CA-PS-Thy-PS-DAP-PS-Br (12). Into a 50 mL Schlenk tube, styrene (5.9 mL, 51.5 mmol), PMDETA (9 μL, 0.043 mmol) and **11** (0.373 g, 0.043 mmol) in 2.95 mL of anisole were added and the reaction mixture was degassed by three freeze–pump–thaw cycles and left under argon. CuBr (6.1 mg, 0.043 mmol) was added to the solution under argon flow. The tube was subsequently placed in a thermostatted oil bath at 110 °C for 40 min. The crude polymer was purified and dried as described above for **8** to give **12** as a white solid (570 mg). $M_{n,SEC}$ = 14 300 Da and PDI = 1.16. Subsequently, the terminal bromide of polymer **12** was converted to the azide functionality as described above for **8**. ATR-IR (cm^{-1}): 2095 (N_3 stretching). $M_{n,SEC}$ = 14 200 Da and PDI = 1.17 (end group fidelity 100%).

Synthesis of CA-PS-Thy-PS-DAP-PS-HW (14). The polymer CA-PS-Thy-PS-DAP-PS-azide (450 mg, 0.031 mmol), compound **13** (65 mg, 0.093 mmol), copper(II) sulfate pentahydrate (23 mg, 0.093 mmol) and sodium ascorbate (19 mg, 0.093 mmol) were dissolved in DMF (10 mL). The resulting mixture was stirred at ambient temperature for 24 h. The crude polymer was purified and dried as described above for **9** to give **14** as white solid. $M_{n,SEC}$ = 15 400 Da, PDI = 1.12. For an end group fidelity assessment refer to Table 1.

Result and discussion

In the following the synthesis of the dual self-folding system will be discussed in detail, inclusive of an assessment of the pairwise orthogonal nature of the recognition units. The synthetic section is followed by the investigation of the single chain self-assembly process itself. The self-assembly section can be read independently of the synthetic part.

Synthesis of the dual self-folding system and orthogonality assessment

A well-defined dual foldable polymer was sequentially prepared by atom transfer radical polymerization (ATRP) and modular ligation chemistry, which permitted the inclusion of defined folding/unfolding points along the backbone mimicking—on a simple level—a natural protein. The resulting polymer contains two competitive yet pairwise orthogonal hydrogen-bonding pairs. The hydrogen bonding recognition units were based on the three-point thymine–diaminopyridine and the six-point cyanuric acid–Hamilton wedge interactions. The selection of these two pairs is driven by the fact that the selected recognition units must be orthogonal to each other, *i.e.* no cross-association should take place. The four pair-wise selected hydrogen-bonding motifs are—to the best of our knowledge—the only combination that fulfils this criterion.[42] It is important to note that the

Table 1 Reaction conditions for the ATRP processes and the properties of the generated polymers, alongside the characteristics of the polymers modified *via* modular conjugation

Polymer	Monomer	$[M_0]/[I_0]$	Init.	Time/min	M_n[b]	M_w/M_n	M_n[c]	Funct.[d]
8[a]	Styrene	200	**7**	30	3000	1.07	3100	100%
9	*Modular ligation of polymer-azide*[e] *and* **6**				3900	1.04	3700	98%
10[a]	Styrene	1000	**9**	60	7700	1.11	7900	90%
11	*Modular ligation of polymer-azide*[f] *and* **3**				8800	1.11	8700	91%
12[a]	Styrene	1200	**11**	40	14 300	1.16	—[h]	—
14	*Modular ligation of polymer-azide*[g] *and* **13**				15 400	1.12	—[h]	—[i]

[a] $[I]_0/[PMDETA]_0/[CuBr]_0 = 1:1:1$; at 110 °C. [b] Determined *via* RI detection SEC using linear **PS standards**. [c] Determined from ^{1}H NMR spectroscopy. [d] Degree of end group functionalization. More details can be found both in the text and the ESI (Fig. S4 and S6–S8†). [e] CA-PS-azide. [f] CA-PS-Thy-PS-azide. [g] CA-PS-Thy-PS-DAP-PS-azide. [h] The end group fidelity of **12** cannot be calculated using ^{1}H NMR due to the absence of a separate, non-overlapping peak to compare with the ω-C*H*Br protons of **12**. [i] Due to the absence of a separate peak, it is not possible to calculate the functionalization fidelity. However, based on the efficiency of the previous transformations (which incur an average functionalization loss of 2 to 3% per step), it is expected to be close to 85% for **14**, given the fact that two additional transformations have been carried out going from **11** to **14**.

thymine–diaminopyridine features weaker binding than the cyanuric acid–Hamilton wedge system (see below for quantitative binding constant data determined on these systems). However, we will demonstrate that these interactions—which are frequently employed in H-bonding driven polymer assembly—are sufficient to induce single chain self-assembly. Our target system was designed to feature a cyanuric acid functional group at the α-position, bearing a thymine and a diaminopyridine functionality at a pre-selected position on the polymer backbone as well as the Hamilton wedge functionality at the ω-position of the single polymer chain (see Scheme 1). To tether these functionalities to a single polymer backbone, a cyanuric acid ATRP initiator, linkers bearing a thymine or diaminopyridine, and the alkyne–Hamilton wedge had to first be synthesized. The detailed characterization of the cyanuric acid functional ATRP initiator, the diaminopyridine with carboxylic acid group and the Hamilton wedge with alkyne group can be found in our previously published procedures.[16,17] ^{1}H NMR spectra of the trifunctional linker compound (see Fig. S1†) and the thymine with ester group (see Fig. S2) can be found in the ESI†.

First, a diaminopyridine compound bearing was synthesized *via* esterification of compound **1** with **2** in the presence of DCC/DMAP as catalysts and DCM/DMF as solvents. The ^{1}H NMR spectrum of **3** indicates that the proton signal corresponding to COO*H* has disappeared and new characteristic proton signals for the CCCH_2O and C(CH_3)Br are observed at 4.75 ppm and 1.88 ppm, respectively (see Fig. 1). Subsequently, the hydrolysis of the methyl ester group of **4** was readily accomplished in the presence of 1 N NaOH in a THF/methanol (2/1) mixture. The hydrolytic success was confirmed by ^{1}H-NMR which indicates that the proton signal from the carboxylic acid of **5** can be observed at 12.58 ppm and the proton signal for the methyl group can no longer be seen at 3.80 ppm (see Fig. S3 in the ESI†). The compound bearing a thymine group was synthesized by esterification of compound **2** with compound **5** in the presence of DCC/DMAP as catalysts and DCM/DMF as solvents. The ^{1}H NMR spectrum of **6** indicates that the proton signal corresponding to COO*H* has disappeared and new characteristic proton signals for CCCH_2O and C(CH_3)Br are observed at 4.75 ppm and 1.88 ppm, respectively (see Fig. 2). The structures of the compounds bearing either thymine or diaminopyridine were also confirmed by ^{13}C NMR and ESI-MS.

Before discussing the synthesis of the single polymer chains with two complementary yet orthogonal recognition pairs at specific positions on the polymer chain (**14**), it is mandatory to investigate the orthogonality of these recognition units to one another *via* their small (denoted with the prefix 's') molecule

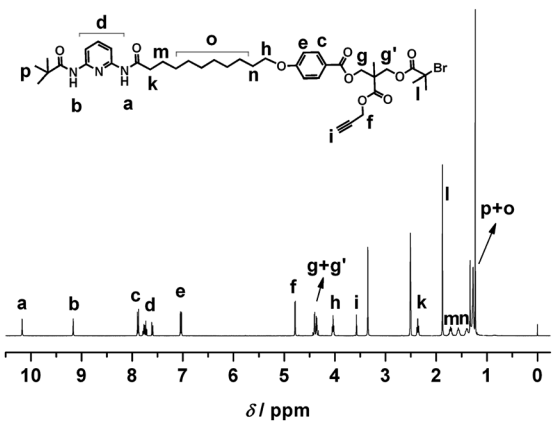

Fig. 1 ^{1}H-NMR spectrum of 2-((2-bromo-2-methylpropanoyloxy) methyl)-2-methyl-3-oxo-3-(prop-2-ynyloxy)propyl 11-(5-methyl-2,4-dioxo-3,4-dihydropyrimidin-1(2*H*)-yl) undecanoate (**3**) in DMSO-d_6.

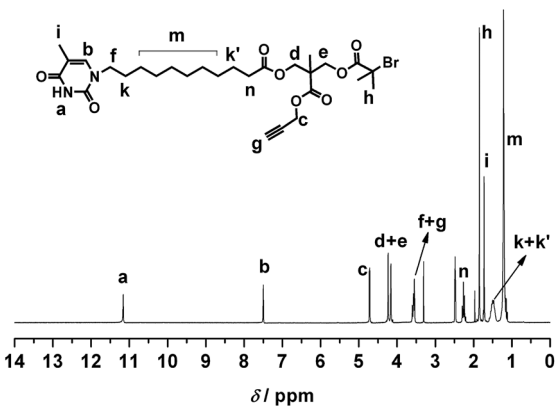

Fig. 2 ^{1}H-NMR spectrum of 2-((2-bromo-2-methylpropanoyloxy) methyl)-2-methyl-3-oxo-3-(prop-2-ynyloxy)propyl 11-(5-methyl-2,4-dioxo-3,4-dihydropyrimidin-1(2*H*)-yl) unde-canoate (**6**) in DMSO-d_6.

analogues (sThy, sCA, sDAP, sHW). The orthogonality of cyanuric acid, the Hamilton wedge, thymine and diaminopyridine has been demonstrated previously by ^{1}H NMR spectroscopy between a pendant functional polymer and small molecules, yet not in their small molecule state.[42] The orthogonality of the functional recognition units was evidenced in the current study by ^{1}H NMR spectroscopy in deuterated dichloromethane (CD_2Cl_2)[33] solution at the ambient temperature. The self-assembly studies were carried out with the following compounds: sDAP (**3**) (see Scheme 2 for a structural imagine), sThy (**6**) (see Scheme 2 for a structural imagine), sCA (**7**) (see Scheme 3 for a structural imagine) and sHW (**13**) (see Scheme 4 for structural imagine). The ^{1}H NMR spectra of sThy (**6**) and sCA (**7**) were independently measured in CD_2Cl_2 at ambient temperature and the NH protons of sThy and sCA were assigned to peaks at 9.07 ppm and 8.81 ppm, respectively (Fig. 3a for sThy and Fig. 3b for sCA). Upon the addition of 1 equiv. of sThy to the solution containing 1 equiv. of sCA, the ^{1}H NMR spectrum of the mixture of sThy and sCA revealed that there is no interaction between these molecules, however, there is a small shift of the NH signals of sThy and sCA and the signals appear at 9.00 and 8.88 ppm, respectively (see Fig. 1c). Next, upon the addition of 1 equiv. of sDAP (**3**) to 1 equiv. of sHW (**13**), the ^{1}H NMR spectrum of the mixture of sDAP and sHW reveals that there is no interaction between sDAP and sHW (see Fig. 1d). When adding 1 equiv. of sDAP to a mixture of 1 equiv. each of sThy and sCA, the ^{1}H NMR spectrum of the sDAP-sThy complex reveals a shift of the imide protons of sThy from 9.00 ppm to 9.52 ppm as well as new proton signals of the complexed sDAP at 8.11 and 8.21 ppm. The NH protons of sCA were located at 9.14 ppm (see Fig. 1e). Subsequently, the addition of 1 equiv. of sHW to a mixture of sCA and the sDAP-sThy complex results in a strong shift of the imide protons of sCA from 9.14 to 12.38 ppm and a new proton signal of the bound sHW at 9.86 and 9.43 ppm was observed in the ^{1}H NMR spectrum. Furthermore, the NH proton signal of sThy shifts from 9.52 to 9.31 ppm and the NH proton signal of sDAP shifts from 8.11 and 8.21 ppm to the aromatic region (see Fig. 1f). These results demonstrate the orthogonality of both the

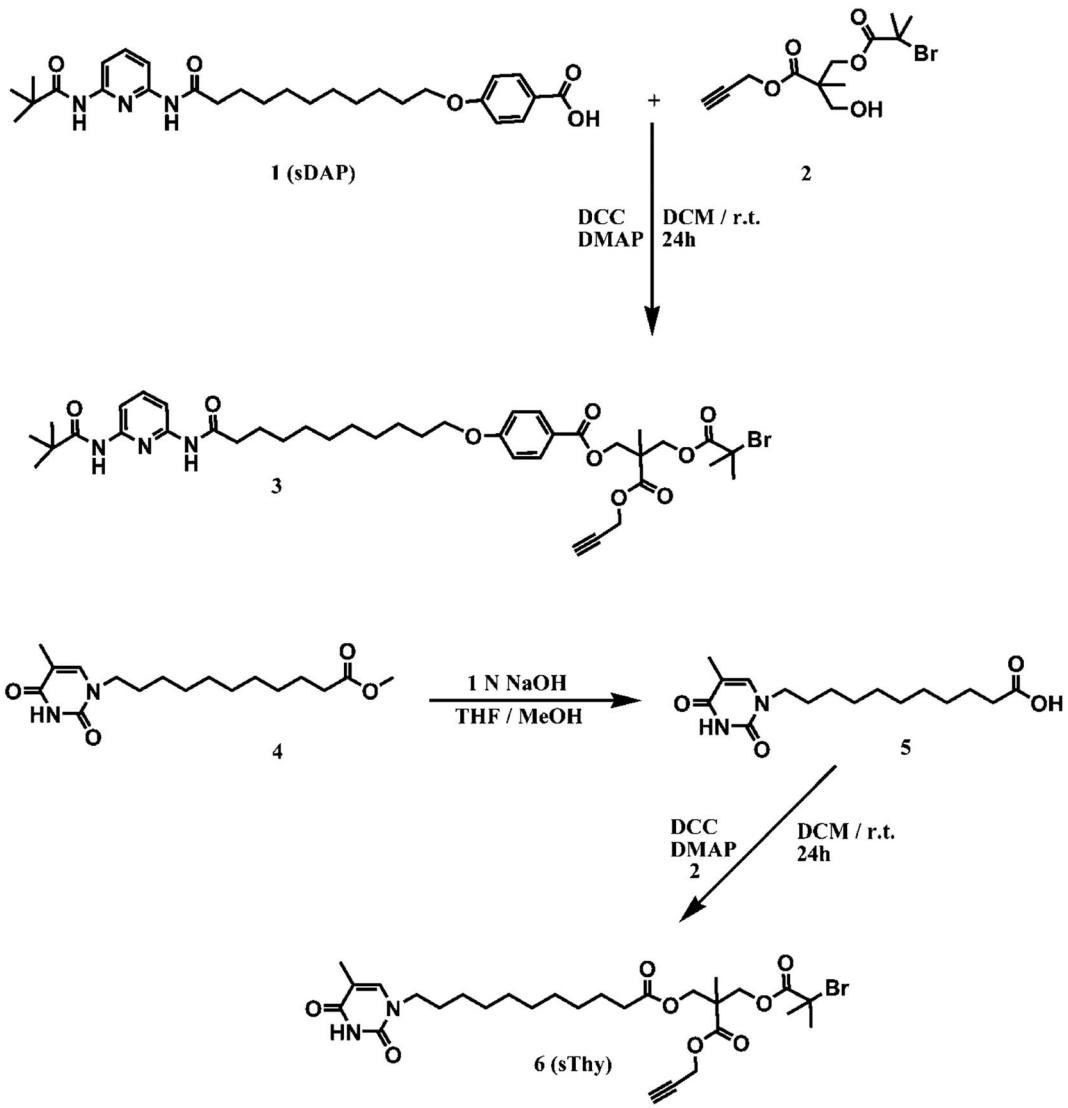

Scheme 2 Synthetic strategy for the preparation of diaminopyridine (sDAP) (**3**) and thymine (sThy) (**6**) bearing linker compounds.

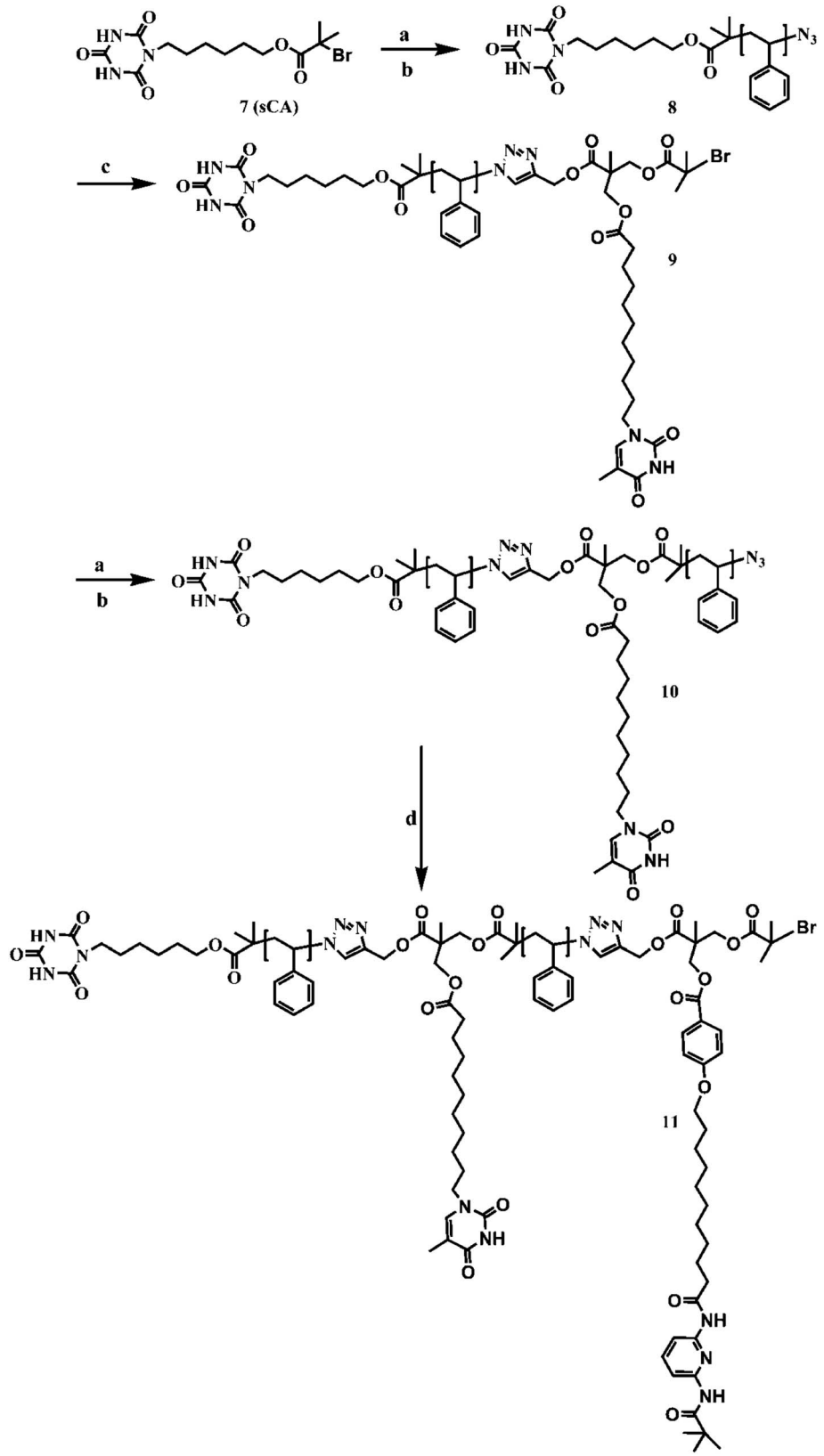

Scheme 3 Synthetic strategy for preparing α-cyanuric acid, thymine bearing and ω-diaminopyridine functional linear polystyrene. *Reagent and conditions*: (a) styrene, CuBr, PMDETA, anisole, 110 °C; (b) NaN_3, DMF, room temperature (rt); (c) $CuSO_4 \cdot 5H_2O$, Na ascorbate, **6**, DMF, rt; (d) $CuSO_4 \cdot 5H_2O$, Na ascorbate, **3**, DMF, rt.

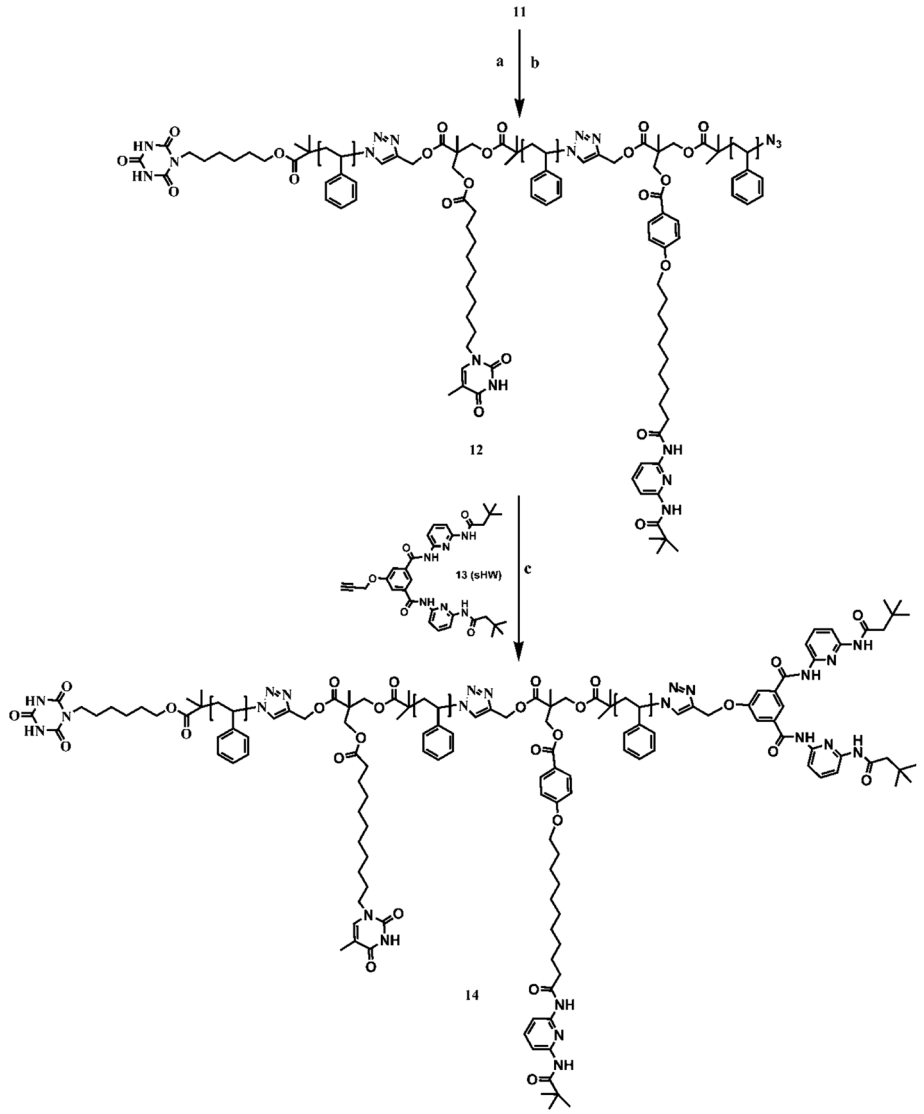

Scheme 4 Synthetic strategy for preparing α-cyanuric acid, thymine and diaminopyridine bearing and ω-Hamilton wedge functional linear polystyrene. *Reagent and conditions*: (a) styrene, CuBr, PMDETA, anisole, 110 °C; (b) NaN_3, DMF, ambient temperature (rt); (c) $CuSO_4 \cdot 5H_2O$, Na ascorbate, **13**, DMF, rt.

three-point sDAP (**3**)–sThy (**6**) and six-point sCA (**7**)–sHW (**13**) interactions on small molecules and evidence no interfering hydrogen-bonding interactions between the two individual recognition pairs. Moreover, the results of these interactions with the small molecules provide useful insights into the NH protons signal shifts which will aid in the analysis of the precursor and final polymer for the single chain self-assembly.

After the synthesis of the functional small molecules and establishing the orthogonal characteristics of the two recognition pairs, a single polymer chain that contained all these complementary recognition pairs at specific positions in its backbone was designed. ATRP and modular ligation chemistry are the preferred synthetic methodologies for the preparation of the complex polymer chain. Subsequently, the halogen end group of the polymers can readily be converted into an azide group enabling the installation of any desired functionality on the polymer chain-end *via* copper catalyzed azide/alkyne [2 + 3] dipolar cycloaddition.

To incorporate a cyanuric acid motif at the α-end of a polymer, a **CA-PS-Br** (**8**) polystyrene was prepared by using **7** as an initiator in the ATRP of St with anisole as the solvent in the presence of a CuBr/PMDETA catalytic system at 110 °C for 30 min. The end group fidelity of **8** (*i.e.* the percentage of chains featuring both a cyanuric acid and bromide terminus) is almost quantitative (calculated from the integral areas of the α-cyanuric acid imide and ω-C*H*Br protons) in the CA-PS-Br (see Fig. S4 in the ESI†). The NMR derived number average molecular weight ($M_{n,NMR} = DP_{n,NMR} \times 104.15$ g mol^{-1} + 377 g mol^{-1} = 26 × 104.15 + 377 = 3100 g mol^{-1}) of CA-PS-Br was calculated by comparing the integrated areas of the aromatic protons of PS at 6.5–7.5 ppm and the two protons of the cyanuric acid end group at 7.91 ppm. It was found that $M_{n,NMR}$ was consistent with the number average molecular weight from SEC ($M_{n,SEC}$ = 3000 Da with M_w/M_n = 1.06) relative to **PS standards**. The ω-bromide end group of the polymer was quantitatively converted into an azide with NaN_3 in DMF at ambient temperature. From the ^{1}H

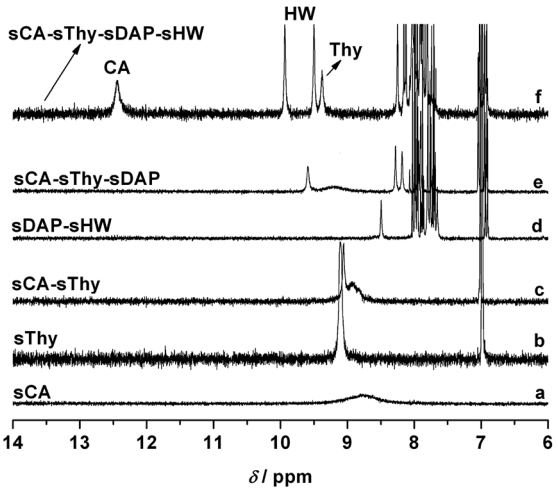

Fig. 3 ^{1}H NMR spectra demonstrating the mutually orthogonal hydrogen bonding of Thy–DAP and CA–HW in CD_2Cl_2 at the ambient temperature. (a) sCA (**7**), (b) sThy (**5**), (c) sCA-sThy (**5** + **7**), (d) sDAP-sHW (**3** + **13**), (e) sCA-sThy-sDAP (**7** + **6** + **13**), (f) sCA-sThy-sDAP-sHW (**7** + **6** + **3** + **13**). The concentration of all recognition units was kept constant at 1 mM.

NMR spectrum of **CA-PS-azide** (see Fig. S5 in the ESI†), it was observed that a signal at 4.5–4.4 corresponding to C*H*–Br at the ω-end of the polymer had completely disappeared and a new signal of the C*H*–N_3 was detected at 3.94 ppm ($M_{n,SEC}$ = 3000 Da with M_w/M_n = 1.06). Subsequently, copper catalyzed azide–alkyne conjugation chemistry was employed to couple the **CA-PS-azide** and compound **6** in the presence of $CuSO_4 \cdot H_2O$/sodium ascorbate in DMF at ambient temperature to give the corresponding **CA-PS-Thy** (**9**) hetero-functional macroinitiator. The number average molecular weights ($M_{n,NMR} = DP_{n,NMR} \times 104.15$ g mol^{-1} + 990 g mol^{-1} = 26 × 104.15 × 990 = 3700 g mol^{-1}) and ($M_{n,SEC}$ = 3900 with M_w/M_n = 1.04) of **CA-PS-Thy** (**9**) were determined *via* ^{1}H NMR and SEC (relative to linear **PS standards**), respectively. From the ^{1}H NMR spectrum of **9**, it can be observed that a signal at 3.9 corresponding to C*H*–N_3 of the ω-end of the polymer had completely disappeared and new signals of the CH_2 and C*H* next to triazole ring were detected at 5.22 ppm. The corresponding ester protons of **6** were assigned at 4.22 ppm (see Fig. S6 in the ESI†). Moreover, the SEC trace of **9** indicated a clear shift to the higher molecular weight region (from 3000 Da to 3900 Da), confirming the introduction of **6**.

These results indicate that the **CA-PS-Thy** (**9**) macroinitiator was quantitatively synthesized *via* the reaction between the **CA-PS-azide** and compound **6** at ambient temperature. **CA-PS-Thy-PS** (**10**) was prepared by using **9** as a macroinitiator for the ATRP of St with anisole as a solvent and a CuBr/PMDETA catalytic system at 110 °C for 60 min. The SEC elugram for **CA-PS-Thy-PS-Br** (**10**) shows a clear shift to the higher molecular weight region compared with its corresponding polymeric precursor. The end group fidelity is *ca.* 93% (calculated from the integral areas of the imide protons of CA-Thy and ω-C*H*Br protons) in the **CA-PS-Thy-PS-Br** (**10**) (see Fig. S7 in the ESI†). The NMR number average molecular weight ($M_{n,NMR} = DP_{n,NMR} \times 104.15$ g mol^{-1} + 990 g mol^{-1} = 67 × 104.15 × 990 = 7900 g mol^{-1}) of **CA-PS-Thy-PS-Br** (**10**) was calculated by comparing the integrated areas of the aromatic protons of PS at 6.5–7.5 ppm and the three protons of cyanuric acid and thymine imide protons at 7.96–8.22 ppm. It is found that $M_{n,NMR}$ was consistent with the number-average molecular weight from SEC ($M_{n,SEC}$ = 7700 Da with M_w/M_n = 1.11). The ω-bromide end group of the polymer was quantitatively converted into an azide in a similar fashion as **8**.

The ^{1}H NMR spectrum of **CA-PS-Thy-PS-azide** indicates that a signal at 4.4 corresponding to C*H*–Br of ω-end of the polymer had disappeared (see Fig. S8 in the ESI†). Next, the copper catalyzed azide–alkyne conjugation was undertaken to couple the **CA-PS-Thy-PS-azide** and compound **3** in the same fashion as **9** to give the corresponding **CA-PS-Thy-PS-DAP** heterofunctional macroinitiator. The ^{1}H NMR spectrum of **CA-PS-Thy-PS-DAP** (**11**) shows new signals of aromatic protons of **3** at 7.65–7.87 ppm and the corresponding ester protons at 4.28–4.33 ppm of **3** (see Fig. S9 in the ESI†). The SEC trace for **CA-PS-Thy-PS-DAP** (**11**) was clearly shifted to the higher molecular weight region (from 7700 Da to 8800 Da), confirming the introduction of the small molecule **3**. Subsequently, **CA-PS-Thy-PS-DAP-PS-Br** (**12**) was prepared by using **11** as a macroinitiator in the ATRP of St with anisole as a solvent and CuBr/PMDETA as the catalyst system 110 °C for 40 min. The degree of end group functionalization of **12** cannot be calculated using ^{1}H NMR, due to the absence of a separate, non-overlapping peak to compare with the ω-C*H*Br protons of **12**. However, it is reasonable to assume that the end group fidelity of **12** was formed in high yield similar to **8** or **10**. The SEC trace for **CA-PS-Thy-PS-DAP-PS-Br** (**12**) is clearly shifted to the higher molecular weight region compared with its corresponding polymeric precursor. The ω-bromide end group of the polymer was quantitatively converted into an azide in a similar fashion to **8** and **10**. Copper catalyzed azide–alkyne conjugation chemistry was subsequently employed to couple the **CA-PS-Thy-PS-DAP-PS-azide** and compound **13** in the same fashion as **9** and **11** to give the corresponding **CA-PS-Thy-PS-DAP-PS-HW** (**14**) hetero-functional polymer chain. The SEC traces (refer to Fig. 4) indicate a clear shift to higher molecular weight region (from 14 300

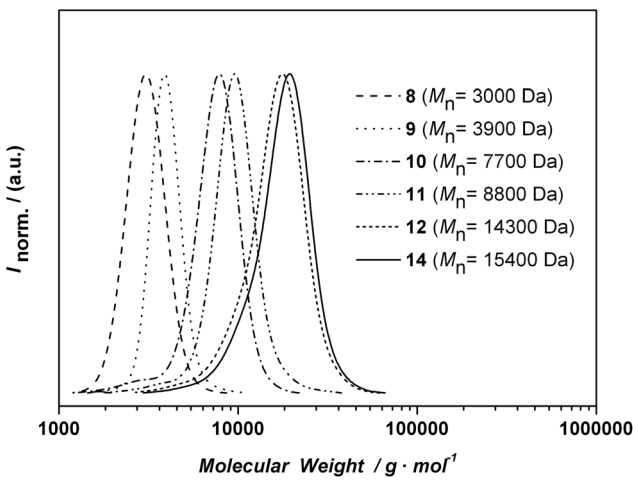

Fig. 4 SEC traces of the precursor polymers and final polymers. The detailed reaction conditions can be found in Table 1. The structural images of the related polymers can be found in Schemes 3 and 4.

Da to 15 400 Da), confirming the introduction of small molecule **13**. Notably, it was observed that all the SEC curves are monomodal with low polydispersity index, thus confirming the introduction of functional small molecules and chain extension of the precursor polymers through ATRP and modular ligation chemistry.

Single chain self-folding of dual hydrogen bonding macromolecules

The characterization of supramolecular polymers is not feasible with most common polymer characterization techniques due to the fact that H-bonding depends on variables such as solvent, concentration, temperature and pressure. However, ^{1}H NMR is an efficient, non-invasive and well-known technique to characterize the H-bonding directed self-assembly of polymers, allowing the study of self-assembly in a wide range of concentrations and temperatures. In addition—and critically important—static and dynamic light scattering are key techniques to study self-assembly processes, especially in the present case where it needs to be established whether *true* single chain self-folding occurs or if higher order agglomerates are formed.

Consequently, evidence for the formation of the efficient assembly of **14** through hydrogen bonding was provided by variable temperature ^{1}H NMR and—most importantly—light scattering methods (SLS and DLS) in CH_2Cl_2 at ambient temperature confirm the single chain self-folding (see below). The hydrogen bond driven self-assembly of a self-folded single polymer chain should lead to a significant down-field shift of the NH protons of the cyanuric acid, Hamilton wedge and thymine moieties. For the ^{1}H NMR studies, a solution of polymer **14** was prepared in CD_2Cl_2 of 1 mM and left for 12 h at ambient temperature to allow for self-assembly. It was observed that the ^{1}H NMR spectrum (see Fig. 5) reveals strong shifts of the amide protons of the Hamilton receptor[33] from 7.80 and 8.52 ppm to 9.35 and 9.78 ppm, respectively. New signals appear at 11.93 and 8.46 ppm that correspond to the bound imide protons of cyanuric acid and thymine, respectively, in the self-assembly motif. However, the bound amide protons of diaminopyridine overlap with the resonances of aromatic protons present in **14**.[28] It should also be noted that the observed chemical shifts are much smaller for the polymeric systems (*i.e.* bound imide protons of cyanuric acid at 11.93 ppm) (see Fig. 5) compared with signals for small molecules (*i.e.* bound imide protons of cyanuric acid at 12.38 ppm) (see Fig. 3), indicating that the presence of the bulky polymeric chains affects the association ability of complementary hydrogen-bonding moieties, possibly due to the altered accessibility within the polymeric system.[17,32]

The temperature and time stability of these hydrogen bonds were additionally investigated *via* ^{1}H NMR. The ^{1}H NMR spectra (see Fig. 5) of the polymer **14** did not show any significant change after prolonged standing (*ca.* 7 days), an observation which revealed that the single chain self-folding of **14** was stable in CD_2Cl_2 solution for long periods. The supramolecular hydrogen-bonded assemblies undergo continuous self-assembly and disassembly processes; the dynamic character of these systems can be revealed by temperature dependent ^{1}H NMR spectroscopy.[44] For temperature based ^{1}H NMR studies, a solution of **14** was prepared in [D_2]tetrachloroethane at a concentration of 1 mM and left for 12 h at ambient temperature to allow for self-assembly. When the solution is heated from −30 to 110 °C, the ^{1}H NMR spectra (see Fig. 6) show a significant down-field shift of the resonances associated with the protons that undergo self-assembly (starting at 13.4 ppm for **CA**, at 10.11 and 9.56 for **HW**, and at 9.10 ppm for **Thy** of polymer **14** at −30 °C due to the stronger associations between the recognition units).[44] These results suggest that at low temperatures the association–dissociation equilibrium is slow on the NMR time scale. Moreover, it can be concluded that by lowering the temperature the

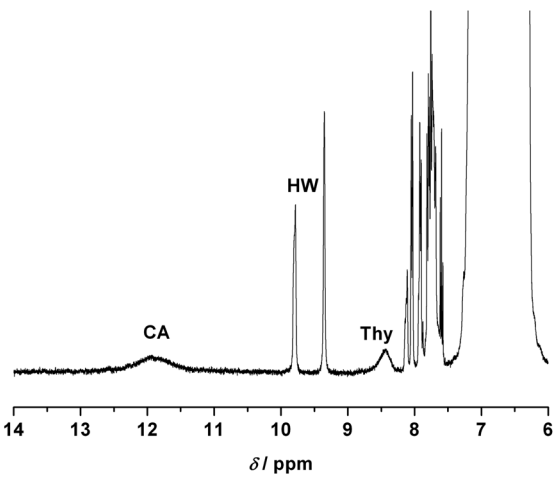

Fig. 5 Expanded ^{1}H NMR of (single chain) self-folded of the polymer **14** (proven by DLS and SLS, see below) in CD_2Cl_2 at ambient temperature showing bound imide protons of cyanuric acid (CA) and thymine (Thy) as well as amide protons of the Hamilton wedge (HW). The bound amide protons of diaminopyridine (DAP) are overlapping with aromatic protons. The concentration of polymer **14** was kept constant at 1 mM.

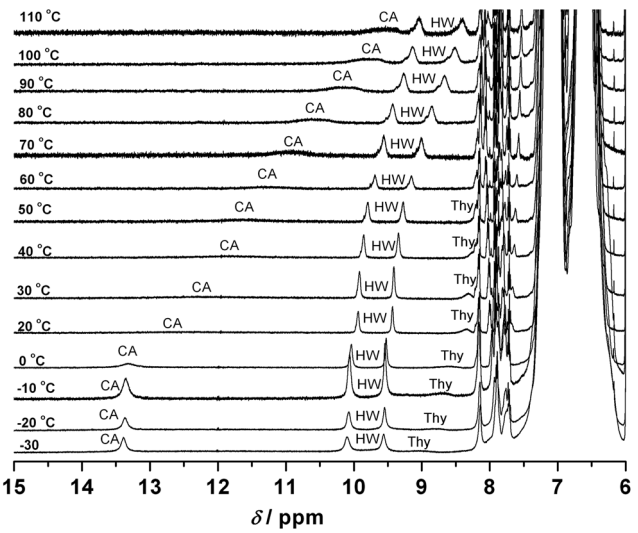

Fig. 6 Expanded ^{1}H NMR of single chain self-folding of the polymer **14** (proven by DLS and SLS, see text) in [D_2]tetrachloroethane at variable temperatures showing bound imide protons of cyanuric acid (CA) and thymine (Thy) as well as amide protons of the Hamilton wedge (HW). The concentration of polymer **14** was kept constant at 1 mM. Note that upon magnification the CA imide protons between +30 and +60 are clearly visible as a broad signal (refer to the ESI, Fig. S11†).

thermodynamic equilibrium is shifted towards the self-folded species and indicates the formation of stabilized structures.[45] It is also evident from Fig. 6 that in the temperature range between +20 and +50 °C the imide protons of **CA** and between 0 and −30 °C the imide protons of **Thy** are in a coalescence regime, where the signals of the bounded NH protons are very broad or cannot be detected anymore.[45,46] The up-field shift of these signals upon increasing the temperature indicates the decreasing stability of the self-folded single polymer chain.[44,45] When the solution of polymer **14** is cooled (inside the NMR probe head) from −110 to −30 °C, the same NMR spectra as depicted in Fig. 6 are obtained. Thus, the changing chemical shifts for the imide protons of **14** evidence the gradual reversibility of the single chain folding/unfolding process as a function of temperature. Furthermore, an earlier reported and established mathematical model[32,47] was employed to deduce the binding constants (K_{ass}) between Thy and DAP, which were found to be close to 653 M^{-1} for the Thy–DAP and 2.4 × 10^6 M^{-1} for the CA–HW system (refer to the ESI† for a detailed description of the process based on our own data from[17]). The six-point hydrogen bonding (CA–HW) exhibits—not surprisingly—significantly larger binding interactions between host and guest than the three-point hydrogen bonding system (Thy–DAP). These binding constants are in the range of those observed and successfully employed in typical H-bonding polymeric systems. For example, the K_{ass} of the H-bonding polymeric chains in halogenated solvents are between 10^2 and 10^3 M^{-1} for the Thy–DAP and between 10^6 and 10^7 M^{-1} for the CA–HW system, respectively.[32,48] In addition, it is important to establish if **14** can be folded and unfolded at will and the switch can be observed *via* ^{1}H-NMR. The disassembly of **14** can be achieved by adding a co-solvent that perturbs the hydrogen bond formation such as methanol.[49] After recording an ^{1}H NMR spectrum of polymer **14** (see Fig. 5) in CD_2Cl_2 in 1 mM concentration, 7 μL of d-methanol (approximately one drop, leading to a methanol concentration of 0.17 mol L^{-1}) were added to the solution and the ^{1}H NMR spectrum (see Fig. S12 in the ESI†) was recorded again. Inspection of Fig. S12† clearly indicates that no resonances are visible anymore between 8.5 ppm and 13.5 ppm corresponding to the protons of Thy, HW and CA in their bound state (compare to the spectrum depicted in Fig. 5).

While ^{1}H NMR is very useful to assess the magnitude of the association process, only light scattering techniques can provide information about the single chain folded nature of the bio-inspired material **14**. *Via* static light scattering (SLS) it is possible to demonstrate that the molecular weight of polymer **14** at high dilutions corresponds to the molecular weight determined *via* SEC analysis of the same polymer. Such an observation implies that polymer **14** is a truly single chain folded system, as otherwise a higher molecular weight—caused by chain–chain association—would be observed.

SLS provides information on the time-averaged properties of the system. The apparent weight average molecular weight (M_w) can be obtained by the Debye relationship:

$$\frac{KC}{I_r} = \frac{1}{M_w}\left(1 + \frac{R_g^2 q^2}{3}\right) + 2A_2C \qquad (1)$$

where C is the concentration (in g L^{-1}), I_r is the relative excess scattering intensity, K is gathered optical parameters, R_g is the radius of gyration, q is the scattering wave vector, and A_2 is the second virial coefficient. The M_w was obtained by extrapolating KC/I_r values to $q = 0$ and $C = 0$ according to eqn 1 (see Fig. S14 in the ESI† for Zimm-Plot for polymer **14** in dichloromethane). SLS obtained molecular weights are collected in Table 2, alongside the SEC determined numbers. Inspection of Table 2 immediately demonstrates that the SEC in THF and SLS in dichloromethane determined molecular weight averages are identical for polymer **14**. In addition, we have also determined the weight average molecular weight of **14** in dichloromethane with a small amount of methanol (7 μL), in which the same value is obtained as in dichloromethane alone. The reason for adding methanol will be detailed in the below DLS section. The SLS measurements are benchmarked against polystyrene (PS) standards (M_w = 17 500 g mol^{-1}), which are also included in Table 2. Furthermore (see Table 2), one can notice a difference in the value of the second virial coefficient A_2—which characterize the interactions polymer/solvent—between the polystyrene standard and polymer **14**. The value of A_2 turns from positive for PS to negative for polymer **14** caused by the presence of the complementary recognition units.

Dynamic light scattering (DLS) has developed into a powerful and versatile tool for estimating the size distribution profile of small particles in suspension or polymers in solution, effective for particles in the size range of a few nanometres up to several micrometres. As a crucial assessment of the efficient formation of self-folded single polymer chains through H-bonding, comparative DLS analyses were performed in dichloromethane solution. Although the above NMR and SLS experiments suggest that stabilized double cyclic structures occur—due to entropy driven self-assembly—only the measurement of the mean hydrodynamic diameter (D_h, which is the volume weight diameter of the distribution) at variable concentrations can provide unequivocal evidence for single chain circular self-folding.[16,17]

Mono-modal particle size distributions could be detected for 1 mM (see Fig. 7) and 2 mM (see Fig. S10 in the ESI†) solutions of **14**, indicating that—at low concentrations—the predominant species were the single chain self-folded polymers. The D_h of the polymers in these solutions were measured to be 8.0 nm and 8.1 nm at 1 mM and 2 mM, respectively. When the concentration was increased to 3 mM, two signal clusters were observed, a major peak at 8.0 nm and a secondary peak at 17.4 nm (see Fig. 8). The percentage fractions of this mixture were calculated to be *ca.* 87% and *ca.* 13%, respectively. Thus, intermolecular interactions were observed at 3 mM solution of polymer **14**, which evidences that the formation of single chain self-folding of the polymer is dependent on concentration; at higher concentrations dual chain aggregates appear. The size distribution

Table 2 Characteristics of polystyrene standard and polymer **14** determined by SEC in THF and by SLS in dichloromethane (DCM)

Polymer	M_n^{SEC}/Da	M_w^{SEC}/Da	M_w^{SLS}/Da	A_2^{SLS}/cm^3 mol g^2
PS standard	17 000	17 500	17 600	1.01×10^{-3}
14	15 400	17 250	20 600	-6.36×10^{-4}
			20 400[a]	-6.06×10^{-4}[a]

[a] Determined after adding methanol ($c_{methanol}$ = 0.17 mol L^{-1}) to the DCM solution.

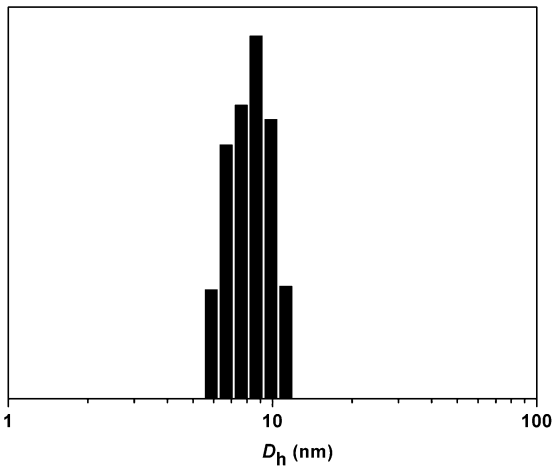

Fig. 7 Mean hydrodynamic diameter of self-folded single polymer chains (**14**) determined at 90°, in 1 mM concentration in dichloromethane at ambient temperature.

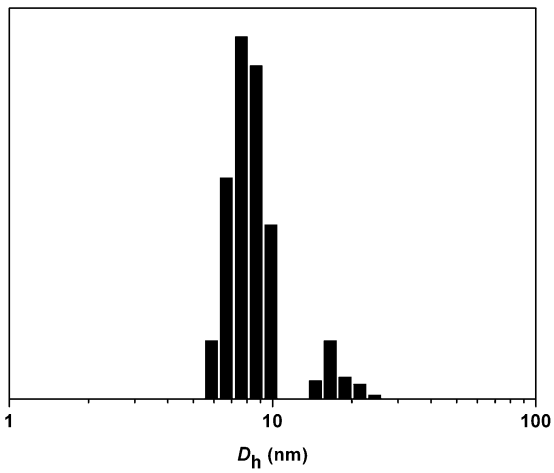

Fig. 8 The mean hydrodynamic diameters of self-folded single polymer chain (**14**) determined at 90°, in 3 mM concentration in dichloromethane at ambient temperature.

obtained at concentrations of 1 and 2 mM of the polymer **14** shows that the mean hydrodynamic diameter of polymer **14** does not change with increasing concentrations which indicates the formation of intra-chain assemblies of **14** at these concentrations. Furthermore, the D_h of a system not capable of folding (*i.e.* **PS standards**, $M_w = 17\ 500$ g mol^{-1}) was also determined by DLS in dichloromethane. The D_h of the **PS standards** was measured as close to 8 nm at variable concentrations. The direct comparison of D_h between pure PS and polymer **14** is not advisable as their structures are very different due to the presence of the large hydrogen bonding recognition units in polymer **14** and consequently their behavior in solution should be different. However—at high concentrations (3 mM)—pure PS does *not* present a bimodal size distribution, which indicates that hydrogen bonding is responsible for the formation of inter-chain assemblies of polymer **14** at high concentrations and thus supports the formation of the more compact single-chain self-folded structures of polymer **14** at low concentrations. The combined ^{1}H NMR and—critically important—the LS results

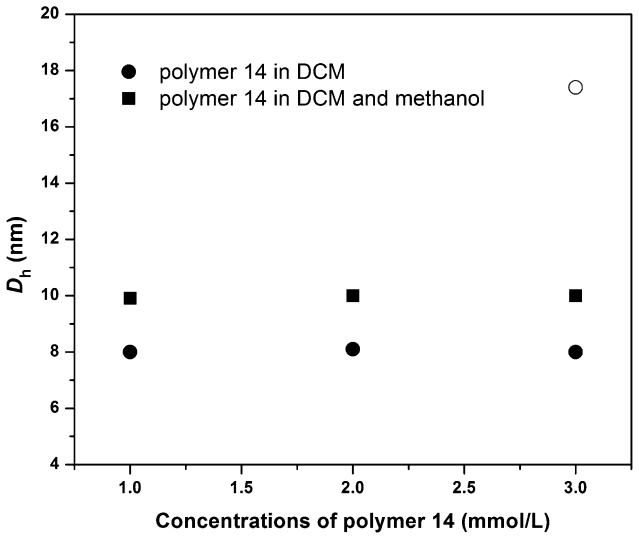

Fig. 9 The mean diameter of the folded structure of polymer **14** in dichloromethane (●) and non-folded structure of polymer **14** in a mixture of dichloromethane and methanol ($c_{methanol} = 0.17$ mol L^{-1}) (■) at different concentrations. Note that at a concentration of 3 mM^{-1} two distributions (open and closed circles) are observed in the system with non-perturbed self-assembly, as higher order structures (not only single chain self-assemblies, *i.e.* chain-chain assemblies) are formed (please also refer to the full distribution data in Fig. 8).

indicate that in dilute solutions stable self-assemblies with a single chain self-folded structure are formed with significantly reduced exchange processes.

Above we have demonstrated that the polymer folding behavior of polymer **14** can be switched at will as evidenced by ^{1}H-NMR spectroscopy (see Fig. S12 in the ESI†). It is now mandatory to carry out DLS measurements to evidence that the D_h also changes upon the addition of the 7 μL of methanol.[49] The DLS measurements are carried out at variable concentrations in CH_2Cl_2 in the presence and absence of methanol (see Fig. 9). The D_h of **14** in these solutions was determined to be 9.9 nm, 10.0 nm, and 10.0 nm (see Fig. S13 in the ESI†), respectively. Upon addition of methanol, the D_h values significantly increase (to 10 nm) as depicted in Fig. 9, whereas no change of the M_w is observed by SLS (see Table 2). This increase is a substantial change in D_h, which is fully congruent with the disappearance of the resonances associated with the H-bonded system (compare Fig. 5 *vs.* S12†). Notably, in the perturbed system higher aggregates are no longer formed as in the non-perturbed system at higher concentrations (see Fig. 9, 3 mM^{-1}). These data thus confirm that polymer **14** features a folded structure in 1 mM and 2 mM solution in CH_2Cl_2 at ambient temperature.

Conclusions

We have for the first time demonstrated the formation of self-folding of a single polymer chain based on two orthogonal non-covalent interactions, *i.e.* a cyanuric acid–Hamilton wedge multiple hydrogen bonding and thymine and diaminopyridine triple hydrogen bonding interaction. Two linker compounds were prepared: 2-((2-bromo-2-methylpropanoyloxy)methyl)-2-methyl-3-oxo-3-(prop-2-ynyloxy)propyl 4-(11-oxo-11-(6-pivalamidopyridin-2-ylamino)undecyloxy)benzoate (**3**), which bears

a diaminopyridine moiety, an alkyne unit, and an initiator for ATRP, as well as 2-((2-bromo-2-methylpropanoyloxy)methyl)-2-methyl-3-oxo-3-(prop-2-ynyloxy)propyl 11-(5-methyl-2,4-dioxo-3,4-dihydropyrimidin-1(2*H*)-yl)undecanoate (**6**), which bears a thymine moiety, an alkyne unit and an initiator for ATRP. The mutual orthogonality of the two recognition units was confirmed by ^{1}H-NMR in CD_2Cl_2 at ambient temperature. Subsequently—starting from a cyanuric acid functional ATRP initiator **7**—a heterofunctional single polymer chain was prepared by ATRP followed by the insertion of a linker compound through modular ligation chemistry. The well-defined precursor macromolecules were characterized *via* both ^{1}H NMR (end group functionalization) and SEC techniques. The self-folding was confirmed by the combination of SLS and DLS data, while temperature dependent ^{1}H NMR provided information about the magnitude and dynamics of the exchange processes. It was found that the single chain self-folding was dependent on concentration and temperature, with single chain self-folded structures dominating—or even exclusively occurring—at low temperatures and high dilution regimes. The construction of even more complex single chain supramolecular polymers and their self-folding studies involving non-covalent interactions based on hydrogen bonds and guided by naturally occurring systems are underway in our laboratories, with the ultimate long term aim of developing synthetic methodologies for the preparation of synthetic protein-like structures that can eventually fulfil biological functions.

Acknowledgements

C.B.-K. is grateful for continued support from the *Karlsruhe Institute of Technology* (KIT) in the context of the *Excellence Initiative* as well as by the German Research Council (DFG) and the Ministry of Science and Arts of the State of Baden-Württemberg. O.A. thanks the Islamic Development Bank (IDB) for a PhD scholarship. The authors are additionally grateful to Dr Nico Dingenouts for assistance with the dynamic light scattering experiments, Dr James Blinco for fruitful discussions and the NMR department of the Institute of Organic Chemistry for their efficient and competent service, especially for the NMR temperature variation measurements.

References and notes

1 C. B. Anfinsen, *Science*, 1973, **181**, 223–230.
2 C. M. Dobson, *Nature*, 2003, **426**, 884–890.
3 D. M. Sadler, *Nature*, 1987, **326**, 174–177.
4 G. Guichard and I. Huc, *Chem. Commun.*, 2011, **47**, 5933–5941.
5 J. Geng, G. Mantovani, L. Tao, J. Nicolas, G. J. Chen, R. Wallis, D. A. Mitchell, B. R. G. Johnson, S. D. Evans and D. M. Haddleton, *J. Am. Chem. Soc.*, 2007, **129**, 15156–15163.
6 K. L. Heredia, T. H. Nguyen, C. W. Chang, V. Bulmus, T. P. Davis and H. D. Maynard, *Chem. Commun.*, 2008, 3245–3247.
7 V. Bulmus, *Polym. Chem.*, 2011, **2**, 1463–1472.
8 P. A. Bertin, J. M. Gibbs, C. K. F. Shen, C. S. Thaxton, W. A. Russin, C. A. Mirkin and S. T. Nguyen, *J. Am. Chem. Soc.*, 2006, **128**, 4168–4169.
9 F. J. Xu and W. T. Yang, *Prog. Polym. Sci.*, 2011, **36**, 1099–1131.
10 K. Matyjaszewski and J. Xia, *Chem. Rev.*, 2001, **101**, 2921–2990.
11 C. J. Hawker, A. W. Bosman and E. Harth, *Chem. Rev.*, 2001, **101**, 3661–3688.
12 G. Moad and C. Barner-Kowollik, in *Handbook of RAFT Polymerization*, ed. C. Barner-Kowollik, Wiley-VCH, Weinheim, 2008.
13 O. Altintas, A. P. Vogt, C. Barner-Kowollik and U. Tunca, *Polym. Chem.*, 2012, **3**, DOI: 10.1039/c1py00249j.
14 H. C. Kolb, M. G. Finn and K. B. Sharpless, *Angew. Chem., Int. Ed.*, 2001, **40**, 2004–2021.
15 C. Barner-Kowollik, F. E. Du Prez, P. Espeel, C. J. Hawker, T. Junkers, H. Schlaad and W. V. Camp, *Angew. Chem., Int. Ed.*, 2011, **50**, 60–62.
16 O. Altintas, P. Gerstel, N. Dingenouts and C. Barner-Kowollik, *Chem. Commun.*, 2010, **46**, 6291–6293.
17 O. Altintas, T. Rudolph and C. Barner-Kowollik, *J. Polym. Sci., Part A: Polym. Chem.*, 2011, **49**, 2566–2576.
18 T. Mes, R. van der Weegen, A. R. A. Palmans and E. W. Meijer, *Angew. Chem., Int. Ed.*, 2011, **50**, 5085–5089.
19 B. V. K. J. Schmidt, N. Fechler, J. Falkenhagen and J.-F. Lutz, *Nat. Chem.*, 2011, **3**, 234–238.
20 L. Brunsveld, B. J. B. Folmer, E. W. Meijer and R. P. Sijbesma, *Chem. Rev.*, 2001, **101**, 4071–4098.
21 J.-M. Lehn, *Chem. Soc. Rev.*, 2007, **36**, 151–160.
22 M. N. Highley, J. M. Pollino, E. Hollembeak and M. Weck, *Chem.–Eur. J.*, 2005, **11**, 2946–2953.
23 O. A. Scherman, G. B. W. L. Ligthart, R. P. Sijbesma and E. W. Meijer, *Angew. Chem., Int. Ed.*, 2006, **45**, 2072–2076.
24 K. E. Feldman, M. J. Kade, T. F. A. de Greef, E. W. Meijer, E. J. Kramer and C. J. Hawker, *Macromolecules*, 2008, **41**, 4694–4700.
25 A. V. Ambade, S. K. Yang and M. Weck, *Angew. Chem., Int. Ed.*, 2009, **48**, 2894–2898.
26 S. K. Yang, A. V. Ambade and M. Weck, *J. Am. Chem. Soc.*, 2010, **132**, 1637–1645.
27 K. E. Feldman, M. J. Kade, E. W. Meijer, E. J. Kramer and C. J. Hawker, *Macromolecules*, 2010, **43**, 5121–5127.
28 A. Bertrand, S. Chen, G. Souharce, C. Ladavieere, E. Fleury and J. Bernard, *Macromolecules*, 2011, **44**, 3694–3704.
29 E. M. Todd and S. C. Zimmerman, *J. Am. Chem. Soc.*, 2007, **129**, 14534–14535.
30 A. Likhitsup, S. Yu, Y.-H. Ng, C. L. L. Chai and E. K. W. Tam, *Chem. Commun.*, 2009, 4070–4072.
31 J. Bernard, F. Lortie and B. Fenet, *Macromol. Rapid Commun.*, 2009, **30**, 83–88.
32 S. Chen, A. Bertrand, X. Chang, P. Alcouffe, C. Ladaviere, J.-F. Gerard, F. Lortie and J. Bernard, *Macromolecules*, 2010, **43**, 5981–5988.
33 O. Altintas, U. Tunca and C. Barner-Kowollik, *Polym. Chem.*, 2011, **2**, 1146–1155.
34 A. T. ten Cate, H. Kooijman, A. L. Spek, R. P. Sijbesma and E. W. Meijer, *J. Am. Chem. Soc.*, 2004, **126**, 3801–3808.
35 E. Harth, B. Van Horn, V. Y. Lee, D. S. Germack, C. P. Gonzales, R. D. Miller and C. J. Hawker, *J. Am. Chem. Soc.*, 2002, **124**, 8653–8660.
36 A. W. Bosman, A. Heumann, G. Klaerner, D. Benoit, J. M. J. Frechet and C. J. Hawker, *J. Am. Chem. Soc.*, 2001, **123**, 6461–6462.
37 T. Terashima, M. Kamigaito, K. Y. Baek, T. Ando and M. Sawamoto, *J. Am. Chem. Soc.*, 2003, **125**, 5288–5289.
38 E. J. Foster, E. B. Berda and E. W. Meijer, *J. Am. Chem. Soc.*, 2009, **131**, 6964–6966.
39 E. B. Berda, E. J. Foster and E. W. Meijer, *Macromolecules*, 2010, **43**, 1430–1437.
40 E. J. Foster, E. B. Berda and E. W. Meijer, *J. Polym. Sci., Part A: Polym. Chem.*, 2011, **49**, 118–126.
41 O. Altintas, G. Hizal and U. Tunca, *J. Polym. Sci., Part A: Polym. Chem.*, 2008, **46**, 1218–1228.
42 C. Burd and M. Weck, *Macromolecules*, 2005, **38**, 7225–7230.
43 O. Altintas, B. Yankul, G. Hizal and U. Tunca, *J. Polym. Sci., Part A: Polym. Chem.*, 2006, **44**, 6458–6465.
44 V. Berl, M. Schmutz, M. J. Krische, R. G. Khoury and J.-M. Lehn, *Chem.–Eur. J.*, 2002, **8**, 1227–1244.
45 K. Hager, A. Franz and A. Hirsch, *Chem.–Eur. J.*, 2006, **12**, 2663–2679.
46 K. Hager, U. Hartnagel and A. Hirsch, *Eur. J. Org. Chem.*, 2007, **2007**, 1942–1956.
47 F. Ilhan, M. Gray and V. M. Rotello, *Macromolecules*, 2001, **34**, 2597–2601.
48 W. H. Binder, M. J. Kunz, C. Kluger, G. Hayn and R. Saf, *Macromolecules*, 2004, **37**, 1749–1759.
49 F. Wessendorf and A. Hirsch, *Tetrahedron*, 2008, **64**, 11480–11489.